Optimization of Phase-Engineered

a-Si:H- Based Multijunction Solar Cells

Christopher R. Wronski, Robert W. Collins,

Joshua Pearce, Jingdong Deng, Vasilios Vlahos,
G. M. Ferreira, C. Chen, and A. Lawrence

Center for Thin Film Devices
The Pennsylvania State University
University Park, PA 16802

Quarterly Technical Status Report
April 2003 – July 2003

Subcontract No. NDJ-1-30630-01

NREL Technical Monitor: Bolko von Roedern

Executive Summary

Task 1. Materials Research and Device Development

Deposition phase diagrams are being developed for VHF PECVD materials in the studies on increasing the deposition rates of Si:H without sacrificing its quality and stability offered by protocrystalline a-Si:H. The effects of the micro-structural changes in a-Si:H materials occurring with increases in deposition rate using RF PECVD on the stability of materials and the performance of solar cells are being investigated. Further improvements in V_{OC} of n-i-p cells are being sought with protocrystalline p-layers having higher doping than the D=0.2 previously used. All the deposition systems are being modified for the fabrication of a-SiGe:H materials and solar cell structures.

Task 3. Device Loss Mechanisms

Studies on carrier transport and recombination, in the dark and under illumination, in p-i-n and n-i-p solar cell structures have been continued. The bulk and interface components are being further characterized and limitations imposed by these two components, as well as p and n contacts on the different solar cell parameters are being investigated using a variety of solar cell structures. The ability to quantify the recombination in the bulk i-layers from J_D-V characteristics, as previously reported, is proving to be extremely useful in establishing the respective limitations. Because of the exponential effect of the mobility gap, E_μ, on carrier recombination and thus the effect on V_{OC}, these studies have been extended to different a-Si:H materials. This includes undiluted R=0, a-Si:H, which have E_μ=1.78 eV, as compared with 1.86 eV of the R=10 protocrystalline materials, which have in the annealed states very similar FF's of about 0.72 for cells with 4000 Å i-layers. The role of potential barriers in the i-layers adjacent to the n, p contacts, as previously reported[1], resulting from *high carrier and not defect* concentrations, in determining different cell characteristics is being further investigated.

In the studies on recombination in the i-layers, J_D-V characteristics have been found in p-i-n cells with R=0 i-layers in which bulk recombination is present over a larger voltage range than those with R=10. In these cells the bulk recombination limitations on 1 sun V_{OC}, which is 0.9 V for an intrinsic layer with E_μ=1.78 eV, could be *conclusively* established from both the dependence on thickness as well as their changes due to SWE in the i-layer. Thus far, no evidence is found that these high 1-sun V_{OC} values are limited by the recombination in the tail states as has been proposed[2].

A study of current-voltage characteristics under illumination is being carried out on different cell structures and analyzed with the approach that was successfully applied to J_D-V, and J_{SC}-V_{OC} characteristics[1].

---

[1] NREL Annual Report 2002, Penn State Univ.

[2] K. Zhu, J. Yang, W. Wang, E. A. Schiff, J. Liang, and S. Guha, *Mat. Res. Soc. Proc*. **762**, A3.2.1, 2003.

Task 4. Characterization Strategies for Advanced Materials

The conventional approach of interpreting photoconductive subgap absorption has been extended to include the contributions of multiple light induced defect states in a-Si:H. In the new approach the evolution of the entire absorption spectra, $\alpha(h\upsilon)$, are analyzed rather than just relying on the magnitude at some arbitrary photon energy as is currently done. This overcomes the serious inadequacies of the current approach whose inconsistencies with other results on films as well as solar cells have been overlooked and lead to misleading conclusions being drawn about the *real* stability of novel materials as well as the origin of SWE. Applying this analysis to results on a-Si:H materials with different microstructure two distinctly different light induced defect states have been identified at 1.0 and 1.2eV from the conduction band. In addition, there are considerable differences in the evolution of the two defect states under 1 sun illumination.

The results are consistent with the corresponding electron mobility lifetime products which can be directly correlated with the FF of the corresponding cells[3], and not the magnitude of $\alpha(E)$. Characterization of light induced defect states is being carried out on a-Si:H materials with controlled differences in microstructure which is also being extended to states above midgap. The results obtained with DBP on films on the evolution of the defect states will be compared to those obtained on J_D-V characteristics on corresponding cells with an approach that is currently under development.

[3] J. M. Pearce, R. J. Koval, R.W. Collins, C. R. Wronski, M.M. Al-Jassim, and K.M. Jones, 29th *IEEE Photovoltaic Specialists Conf. Proc.,* (IEEE, 2002) p. 1101.

Task 3. Device loss mechanisms

Limitations of n contacts

There have been many studies focusing on the effect of p-layers on the performance of a-Si:H solar cells. On the other hand, there have been fewer studies on the effect of n-layers and even in such studies on n-layers the explanations of their role in determining the solar cell performance have been somewhat misleading. This is due to the incomplete characterization of their effect on different cell parameters and interpretations based on the presence of large densities of defects in the vicinity of these contacts. In order to obtain further insight into the effect of the potential barrier, V_n, in the i-layer at the n contact due to the high density of electrons there[4]. Studies were carried out on identical a-Si:H p-i-n cell structure but with n-a-Si:H and n-μc-Si:H contacts. The n-a-Si:H material has a mobility gap E_μ of ~ 1.80 eV and activation energy of 0.26 eV and the n-μc-Si:H material has a E_μ of 1.1 eV and activation energy of 30 mV. Figure 1 shows the J_D-V characteristics for both the cells. Clearly seen from the figure, there is excellent overlap between the two characteristics up to around 0.9 V before they diverge which indicates that bulk recombination is the same in both cells[5]. The cell with a-Si:H n-layer exhibits lower current at high forward bias than that does the cell with μc-Si:H n-layer indicating some effective series resistance introduced by incorporating a-Si:H n-layer into the cell. However, although the conductivity of the a-Si:H n-layer is lower than that of the μc-Si:H n-layer, it is still much greater than that of the a-SiC:H p-layer so that the bulk resistance of the n-layer is not the limiting factor in the current transport across the cell. Such an effective series resistance then can be only due to the remaining difference between the two n-layers; positions of E_F in the n contact relative to the conduction band (E_c) of the i-layer, which leads to different magnitude of the current limiting barrier V_n. It has been shown that the offsets between the conduction and the valence bands of a-Si:H and that of μc-Si:H are approximately equal[6], so that E_c of n-μc-Si:H is lower than that of i-a-Si:H by as much as 0.35 eV. However, due to this large conduction band offset, even though the Fermi level E_F is closer to E_c in μc-Si:H n-layer than that in a-Si:H n-layer, it is further away from E_c in the i-layer at the n/i interface of the cell with μc-Si:H n-layer than that in the cell with a-Si:H n-layer. Consequently higher electron concentration in the i-layer near the n/i interface in the cell with a-Si:H n-layer results in a V_n which then imposes a larger limitation on the current across the cell at high forward biases.

[4] J. Deng, J.M. Pearce, V. Vlahos, R.W. Collins, and C.R. Wronski, *Mat. Res. Soc. Proc*. **762**, A3.4.1 (2003).
[5] J. Deng, J.M. Pearce, R.J. Koval, V. Vlahos, R.W. Collins, and C.R. Wronski, *Appl. Phys. Lett*. **82**, 3023 (2003).
[6] R.J. Koval, A.S. Ferlauto, J.M. Pearce, R.W. Collins, and C.R. Wronski, *J. Non. Cryst. Solids*, **299-302**, 1136 (2002)

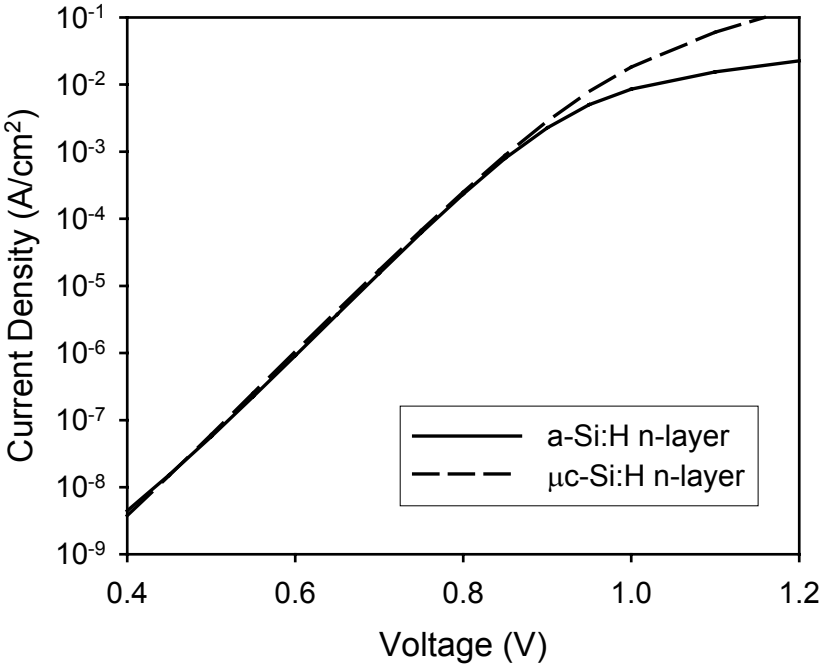

Figure 1. J_D-V characteristics for two p-i-n solar cells having the identical cell structures except one with a-Si:H n-layer and the other with mc-Si:H n-layer.

The limitations imposed by the n/i interface region on the current transport are further verified by the light J-V results. The cell with the a-Si:H n-layer has a FF of 0.68, much lower than that of the cell with μc-Si:H n-layer (0.73). As expected, both of the cells have the same V_{OC} (0.92 V), since at open circuit condition there is no net current flowing through the cell so that there is no current limiting effect from the barrier at the n/i interface. In the work reported recently on the effects that a-Si:H and μc-Si:H n contacts have on V_n, where there were no comparisons made between the J_D-V characteristics, quite misleading conclusions were presented based on results of just V_{OC} and numerical modeling[7]. These included that there is no "gain" from replacing a-Si:H n-layer with the μc-Si:H n-layer and, contrary to our results, that due to the large band discontinuity there is a *larger potential drop* at the n/i interface in the cell with μc-Si:H n-layer instead of in the cell with a-Si:H n-layer.. These conclusions are based on the assumption that V_{OC} is determined by the built-in potential, which is only true when the current transport is completely interface recombination dominated. However, there is no supporting evidence from experimental data, such as J_D-V characteristics, for such an argument. In fact, as will be shown in the next section, 1-sun V_{OC} can be determined by bulk recombination, which is then not affected by the built-in potential so that no conclusion can be drawn about the built-in potential in different cells by just comparing V_{OC}.

[7] Y. Poissant, P. Chatterjee, and P. Roca i Cabarrocas, J. Appl. Phys. **93**, 170, 2003.

Limitation of bulk recombination on 1-sun V_{OC}

In a well designed cell structure with optimized p/i, n/i interfaces and n, p contacts, the current transport in the dark and under illumination are both dominated by the recombination in the bulk of the i-layer. This has been verified with the detailed studies on a series of p-i-n solar cells having R=0 i-layer with different thickness of 0.4μm, 0.8μm, and 1.5μm, respectively. In these cells, the interface recombination has been minimized by incorporating a 200 Å thick R=40 intrinsic layer at the p/i interface. As has been previously reported[8], the J_D-V characteristics of such cells exhibit clear thickness dependence. This is illustrated in Figure 2 together with results that for the *first time clearly* establish the thickness dependence of the V_{OC} in these cells. It is worth stressing here the well recognized fact that both the interface recombination and bulk recombination depend on the carrier concentrations in the i-layer. Because these have an exponential dependence on the mobility gap, E_μ, and the subsequently strong dependence of V_{OC} on E_μ, their values must be taken into account when the comparison is made between V_{OC} s of cells having different i-layers. This unfortunately is not generally done and in particularly when "record" values are being reported or limitations on V_{OC} being proposed from "analysis" based on results on different cells.

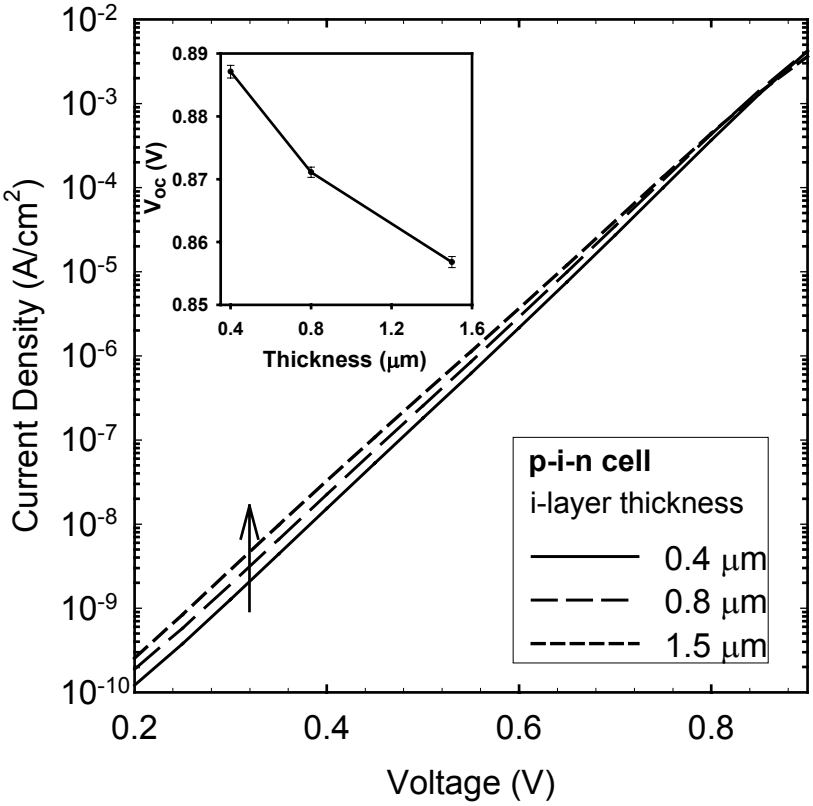

Figure 2. J_D-V characteristics of p-i-n solar cells having R=0 i-layer with different thickness of 0.4mm, 0.8mm, and 1.5mm, respectively. Shown in the inset is the V_{OC}'s of these cells under red light illuminations which induce a constant J_{SC} for all the cells very close to that at 1 sun.

[8] NREL Annual Report 2002, Penn State Univ

In these cells the R=0 i-layer has an E_μ of 1.78eV obtained from internal photoemission measurements. The illumination levels under which the V_{OC}'s were measured were adjusted for each cell so that the J_{SC} (7.5 mA/cm^2) is the same and is very close to the value under 1 sun illumination. From the figure, it is clearly seen that the V_{OC} decreases with the i-layer thickness due to the higher total recombination current in the thicker cells, which confirms the bulk dominance of the recombination current. It is very important to note here that to obtain the thickness dependence of the V_{OC}, the measurements should not be carried out under a constant illumination level for all the cells as has been done in many studies carried on the thickness dependence of V_{OC}. When the illumination is constant for all the cells the total generation current of a thicker cell is higher, which cancels out its higher bulk recombination current so that it will have a similar V_{OC} as that of the thinner cells. This is a possible reason for the reported absence of thickness dependence of V_{OC} which would lead to the wrong conclusions about V_{OC} not being bulk recombination limited even when the interface recombination has been minimized. For example with i-layer thickness of 0.4μm, 0.8μm, in which the thickness dependence of V_{OC} was established here under the condition of constant $J_{SC,}$ have exactly the same V_{OC} (0.906 V) under 1-sun illumination.

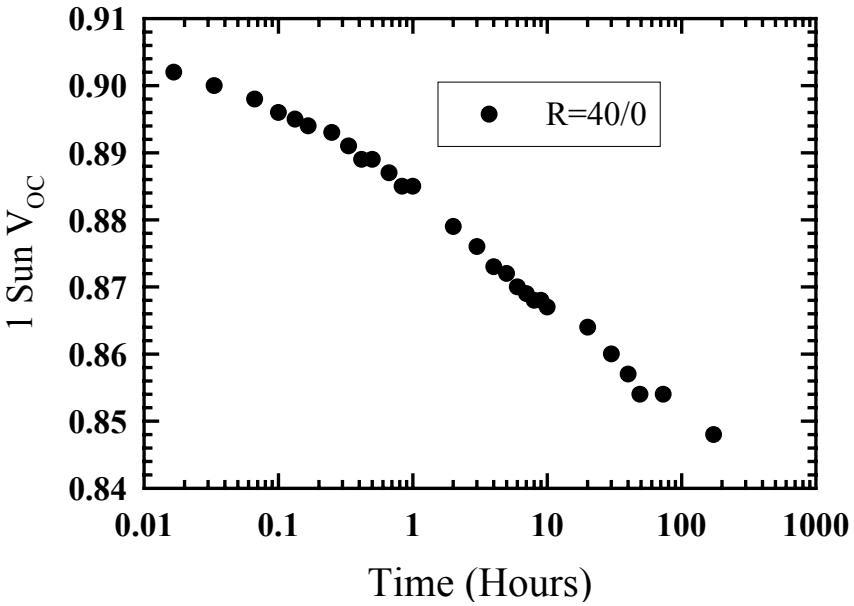

Figure 3. Light induced degradation kinetics of the 1-sun V_{OC} for the cell with 0.4mm thick R=0 i-layer and 200 Å thick R=40 at the p/i interface.

The dominance of V_{OC} by bulk recombination in the cells was further confirmed by the light induced changes (SWE) in the i-layers. Figure 3 shows the light induced degradation kinetics of the 1-sun V_{OC} for the cell with 0.4μm thick i-layer. From the figure, it can be clearly seen that a decrease in V_{OC} occurs instantaneously due to the introduction of the light induced defects and corresponding increase in bulk recombination. In addition to confirming the bulk recombination limitation on V_{OC}, the

results in Figure 3 indicate that the 1-sun V_{OC} is not limited by the tail states since their densities and thus carrier recombination through them does not *increase* due to SWE.

Limitations on FF

Although fill factors are critical parameters for determining the performance of solar cells, they have not been fully characterized due to the complexities associated with the contributions due to the properties of bulk i-layer, p/i, n/i interface regions and n, p contacts. In spite of this, it is still possible to identify and characterize some of the mechanisms determining the FF. In order to investigate these mechanisms an approache has been taken in which carefully designed cell structures are studied under different illumination intensities and some preliminary results are presented here.

For an ideal p-i-n or n-i-p a-Si:H solar cell without any defects and series resistance effects, its FF is only determined by the slope of the light current drop near V_{OC} when the generation current is canceled out by the exponentially growing forward bias current. This slope is determined by both the diode quality factor, n, of the solar cell and the illumination intensity where lower values of n and higher illumination give a higher FF. Consequently, in a cell where n is constant, the FF simply increases with illumination intensity. However, in a-Si:H solar cells, two additional contributions to the FF have to be included: the defect states in the i-layer and effective series resistance. Recombination through the defects reduces the collected photo-generated current and the effective series resistance reduces the carrier collection by reducing the electric field across the bulk i-layer. This effective series resistance can be either due to the bulk resistance of the non-optimized (resistive) n, p contacts, or due to the current limiting barrier formed near the p/i and n/i interface due to the space charge effect, as has been discussed earlier[9].

The effect of illumination intensity on these two contributions is the following. For higher illumination intensities, the increase in quasi-Fermi level splitting results in more gap states acting as recombination centers and the carrier recombination increases by a factor larger than that of the increase in the photo-generated current. At the same time, reduction in the electric field across the bulk caused by the effective series resistance becomes larger as the potential drop across the barriers in the vicinity of the contacts increases due to the higher photo current. Consequently, the observed decreases of the FF at high illumination levels in a-Si:H solar cells are due to these two factors.

Preliminary results shown in Figure 4, where the FF's of the two cells of Figure 1 are plotted versus J_{SC}, indicate the validity of the above discussion and that the approach taken will offer new insights into the factors limiting FF. It can be clearly seen that, as expected, both FF's increase with J_{SC} at the low illumination intensities but decrease with J_{SC} at high illumination intensities. In addition, the FF's for the cell with a-Si:H n-layer are significantly lower at the high illumination intensities than those for the cell with the μc-Si:H n-layer due to the larger current limiting barrier at the n/i interface discussed earlier.

[9] NREL Annual Report 2002, Penn State Univ.

These preliminary results indicate that studies carried out in detail on carefully designed cell structures will lead to a clearer understanding of the bulk, contact and interface limitation on the FF in a-Si:H solar cells.

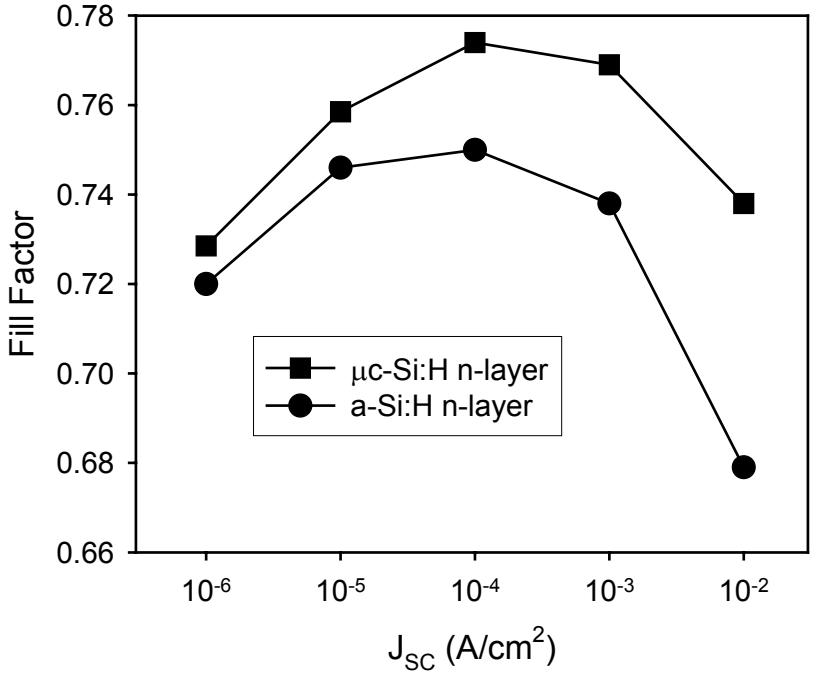

Figure 4. Variation of fill-factors as illumination levels change for the cells in Figure 1.

Task 4: Characterization Strategies for Advanced Materials

The light induced degradation in a-Si:H is generally associated with the creation of dangling bonds and the emphasis has been on determining their evolution under illumination. Although the neutral dangling bond (D^0) defect density can be directly measured with electron spin resonance the most commonly used method is photoconductive subgap absorption as a function of photon energy, $\alpha(h\upsilon)$. Generally $\alpha(h\upsilon)$ is interpreted solely in terms of D^0 defect states where their densities are directly related to the magnitude, $\int \alpha(h\upsilon) \, dh\upsilon$, typically for $h\upsilon$ 1.1 to 1.3eV. Such an approach has been successful in explaining a plethora of results on light induced changes in carrier recombination and their annealing. However, results have also been reported that point to the introduction of other defect states and that $\alpha(h\upsilon)$ cannot be interpreted in such a simple manner.[10] The approach taken in our work is to take into account the contributions to the $\alpha(h\upsilon)$ of multiple defect states by analyzing the evolution of the entire spectra rather than just their magnitude. This has been carried out for states at and below midgap whose direct correlation with carrier recombination is limited by the presence of states above midgap. Nevertheless two distinctly different light induced defect states centered around 1.0eV and 1.2eV from the conduction band edge have been clearly identified where their evolution is found to be consistent with the corresponding changes in the electron $\mu\tau$ products.

An example of this approach is presented here with two materials having radically different microstructure and consequently degradation kinetics. One is a protocrystalline material deposited with $R \equiv [H_2]/[SiH_4] = 10$ at a deposition rate of 0.5Å/s and the other is an undiluted R=0 material deposited at a rate of 20Å/s.[11,12] Shown in Fig. 4.1 are the $\mu\tau$ products at carrier generation rates of $10^{19} cm^{-3} s^{-1}$ for the two materials in the annealed state (AS) and their changes under 1 sun illumination at 25°C. Also shown are the $\mu\tau$ products for the R=10 material at 75°C. It can be seen in Fig. 4.1 that in the AS the $\mu\tau$ product of the R=10 material is about 5 times higher than in the R=0 material, as is generally expected for better quality materials. Although, there is a similarity in the kinetics of their initial light induced changes, there is a marked difference in their evolution towards a degraded steady state (DSS). At 25°C the protocrystalline material attains a DSS in approximately 100 hours whereas in the R=0 the commonly reported kinetics with $\sim t^{-1/3}$ extends for 400 hours with no approach to DSS. It should be noted here that after 150 hours the $\mu\tau$ product are ~10 times higher in the R=10 than in the R=0 material. When the temperature of degradation is raised to 75°C there is virtually no change in the kinetics of the 20Å/s material whereas the R=10 reaches a DSS with a $\mu\tau$ values that is ~2 times higher than at 25°C.

---

[10] C. R. Wronski, J. M. Pearce, R. J. Koval, X. Niu, A. S. Ferlauto, J. Koh, and R. W. Collins, *Mat. Res. Soc. Proc.* **715**, A13.4 (2002).

[11] R. Koval, X. Niu, J. Pearce, L. Jiao, G. Ganguly, J. Yang, S. Guha, R. W. Collins, C. R. Wronski, Mat. Res. Soc. Proc., **609**, A15.5 (2000).

[12] 7. M. Kondo, T. Nishimoto, M. Takai, S. Suzuki, Y. Nasuno, and A. Matsuda, *Technical Digest of the 12th International PV Science and Engineering Conf.* (2001) p. 41.

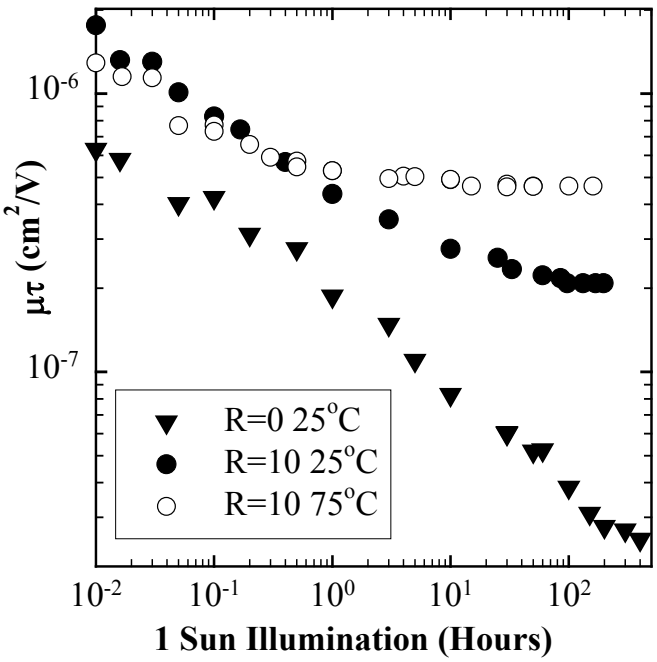

Figure 4.1. Electron mobility lifetime products as a function of exposure to 1 sun illumination time for R=0 and R=10 materials at 25°C and for the R=10 material at 75°C.

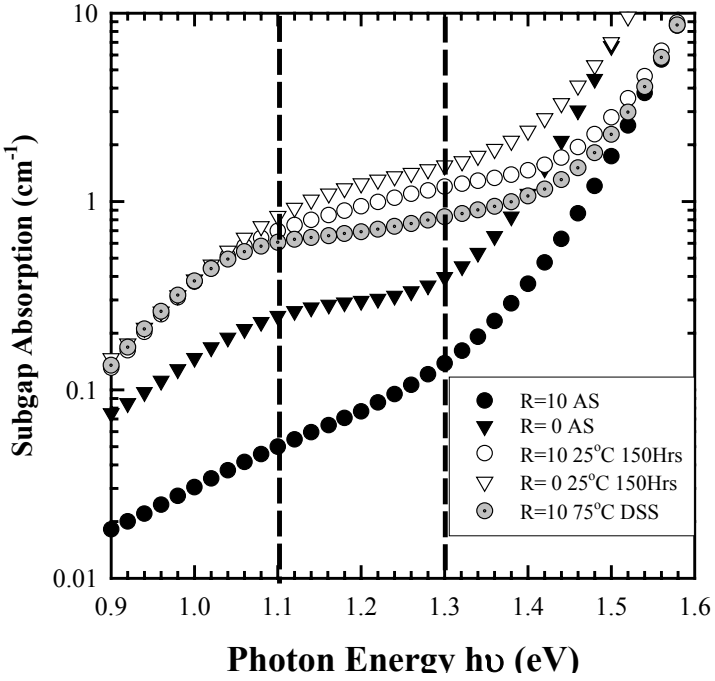

Figure 4.2. Subgap absorption as a function of photon energy for the R=0 and R=10 materials in the annealed state and after 150 hours of 1 sun illumination at 25°C and the R=10 film in a degraded steady state at 75°C.

In Fig. 4.2 the α(hυ) spectra are shown for the two materials in the annealed state, as well as after 150 hrs of degradation at 25°C. Also shown are the results for the DSS of the R=10 film degraded at 75°C. The effects of the valence band states on α(hυ) spectra can be observed above 1.3eV, where the values for the two materials differ because of their bandgaps ($E_{\alpha 2000}$), which are 1.86eV and ~1.80eV for the R=10 and R=0 materials respectively. In the annealed state the $|\alpha(h\upsilon)|$ in the region from 1.1 to 1.3eV, commonly used in evaluating α(E), is ~4 times lower than that of R=0 material. Although this is consistent with the lower values of μτ, it is important to note the striking difference between the shapes of the α(hυ) spectra. The R=0 spectra has the commonly found shoulder whereas, the R=10 continually decreases with hυ due to its protocrystalline nature. This clearly indicates a significant difference in the intrinsic gap states of the two materials other than just their densities.

In the degraded states, the differences between the various spectra are subtler since they have similar values of α(hυ). After 150 hours of illumination at 25°C the R=10 film clearly develops a shoulder similar to that in the R=0 material. The $|\alpha(h\upsilon)|$ values in the region 1.1 to 1.3eV in the two materials are consistent with those of μτ, higher $|\alpha(h\upsilon)|$ values correspond to lower μτ values. However, the small difference of ~30% in α(1.2eV) is completely inconsistent with the difference of a factor of 10 in the μτ products. Similarly the reduction in α(1.2eV) values of the R=10 material in the 75°C DSS is consistent with the corresponding higher values of μτ, but not by the factor of >2. Since for the R=0 material no difference in μτ kinetics is present between 25 and 75°C, as expected there were none in the α(hυ) spectra. It is quite apparent from the results just discussed that the evolution of multiple defect states has to be taken into account in interpreting α(hυ) spectra. This becomes even more evident from the α(hυ) spectra for hυ<1.1eV, which, as can be seen in Fig. 4.2, are virtually identical despite the large differences in the corresponding μτ products.

Any interpretation of α(hυ) in terms of the density and energy distribution of multiple defect states is complicated by the nature of photoconductive subgap absorption, which is determined by N(E), the densities of *electron occupied states and not directly by the total defect density*, N_{DEF}. Photoconductive subgap absorption is determined from the absorption of photons, which excite electrons into the extended states in the conduction band whose density is then measured as the generated photocurrent. Thus, for any given photon energy, α(hυ) is a measure of the number of electrons excited into the conduction band (E_C) which are located within hυ of E_C and is given by [13]:

$$\alpha(h\upsilon) = k(h\upsilon)^{-1} \int N(E) N_{CO}(E+h\upsilon-E_C)^{1/2} dE \qquad (1)$$

The integral takes into account that hυ can excite electrons located $E_C - E < h\upsilon$. $N_{CO}(E-E_C)^{1/2}$ is the parabolic distribution of extended states in the conduction band. k depends on the dipole matrix elements for transitions from localized to extended states and is assumed to be constant.[14] In the case of a single type of defect state it is possible to relate N(E) to $N_{def}(E)$ directly because the occupation of these states is constrained by charge

[13] J. M. Pearce, J. Deng, V. Vlahos, R. W. Collins, and C. R. Wronski, *Proceedings of the 3rd World Conference on Photovoltaic Energy Conversion*, (in press).

[14] W.B. Jackson, S.M. Kelso, C.C. Tsai, J.W. Allen, and S.J. Oh, *Phys. Rev. B* **31**, 5187 (1985).

neutrality. However, in the case of multiple defect states the electron occupation of each type of state is *determined by the kinetics of carrier recombination* and depends not only on their energy distribution in the gap but also on their relative densities and capture cross-sections of the states.[15] Despite these complexities, information can be obtained about the evolution of the light induced defects and in particular their energy distributions. In order to relate $\alpha(h\upsilon)$, which includes the contributions from all the electron occupied states at energies within $h\upsilon$ from E_C, to the energies of the defect states relative to E_C it is necessary to take the derivative of the $\alpha(h\upsilon)$ spectra. In the case when N(E) change rapidly with E, such as a Gaussian distribution, the effect of $N_{CO}(E-E_C)^{1/2}$ on the joint density of states is small. Consequently, the derivative of equation 1 yields:

$$\mathbf{kN(E) = (h\upsilon)d[\alpha(h\upsilon)]/dE - \alpha(h\upsilon)} \qquad \mathbf{(2)}$$

The evolution of the light induced gap states can be characterized by normalizing the values obtained from equation 2 for kN(E) after degradation to that in the annealed state yielding:

$$\mathbf{P(E) = kN_{DS}(E)/kN_{AS}(E) = N_{DS}(E)/N_{AS}(E)} \qquad \mathbf{(3)}$$

The P(E) spectra obtained from the results in Fig. 4.2 are shown in Fig. 4.3 where their magnitude represents the increase in the densities of electron occupied states at different energies in the gap from the annealed state (AS). Because of the complexities mentioned above, quantifying the P(E) spectra in terms of $N_{DEF}(E)$ can not be made without numerical modeling. Nevertheless, it is possible to identify their energy distributions and relate the differences to those in $\mu\tau$, which clearly is not possible for $\left|\alpha(E)\right|$. From the results in Fig. 4.3 the creation of two distinctly different light induced defect states centered around 1.0 and 1.2eV from E_C can be clearly identified. In the case of the R=0 material after 100 hours of degradation at 25°C there is the predominant contribution from the peak around 1.2eV, which dominates the spectrum with an almost negligible tail extending towards midgap. In the case of the protocrystalline material on the other hand, this contribution to the P(E) spectrum is drastically reduced so that there is now a broad peak centered at 1.0eV with only a shoulder at 1.2eV. The creation of large densities of the light induced defect states in the R=0 material around 1.2eV can be attributed to its poor microstructure due to the fast rate deposition rate. Clearly identifying these states and distinguishing them from those around 1.0eV cannot be as readily done in materials deposited at slow rates. This enormous difference in P(1.2eV) between the two films seen in Fig. 4.3 clearly indicates the presence of a large difference in their gap state, which is then reflected in the factor of 10 difference in their corresponding $\mu\tau$ products. A more quantitative comparison can be made between the contributions of the two states from $\left|P(E)\right|$ spectra on the same material under different degradation conditions. It is seen in Fig. 4.3 that for the R=10 material that in the improved DSS at 75°C there is only a slight reduction in the defect states around 1.0eV. The much larger suppression of those around 1.2eV, on the other hand, can explain the $\mu\tau$ values that are a factor of >2 higher. However, since no corresponding information is currently available about the states

[15] A. Rose, Concepts in Photoconductivities and Allied Problems, Robert. E. Kreiger Pub.: New York, 1978.

located above midgap no definite conclusions can be drawn about the nature of these two defect states.

The distinctly different light induced defect states centered around 1.0 and 1.2eV from E_C and their respective effects on carrier recombination, are consistent with a variety of results which cannot be explained in terms of a single state located around midgap. Their evolution is also consistent with the presence of "slow" and "fast" defects[16] as well as the degradation kinetics of a-Si:H films and cells.[17, 18] Since recently direct correlations have been established between the light induced changes in $\mu\tau$ and the FF of corresponding solar cells it is important therefore to take into account the presence of at least these two defect states in evaluating the stability of a-Si:H solar cell materials and not be misled by the simple interpretations of $\alpha(h\upsilon)$ spectra. It is also important to note their distinct differences in their creation kinetics cannot be overlooked in the attempts on establishing the origin of the Staebler-Wronski Effect.

Studies are being carried out on a-Si:H material with different microstructures and characterization of gap states to within 0.5 eV of E_c has been initiated.

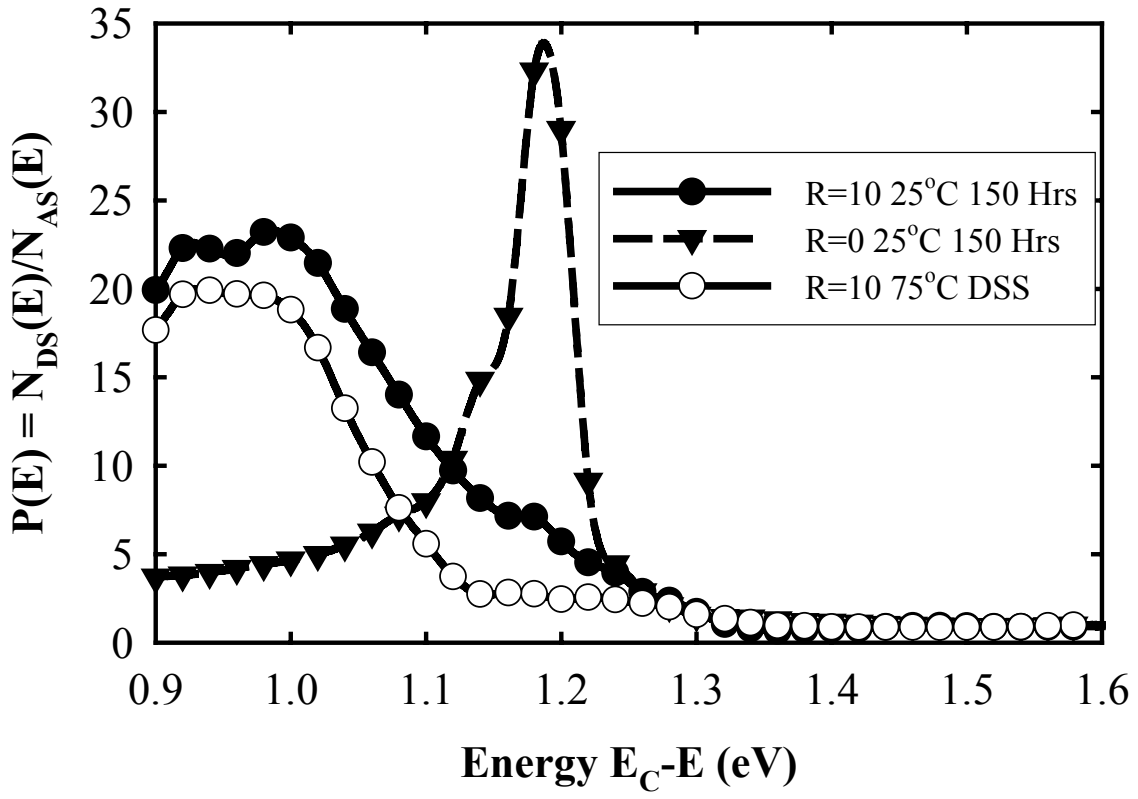

Figure 4.3. The $P(E)= N_{DS}(E)/N_{AS}(E)$ spectra as a function of energy from the conduction band obtained for the results shown in Fig. 4.2.

---

[16] L.Yang and L. Chen, Appl. Phys. Lett. 63, 400 (1993).

[17] J. M. Pearce, R. J. Koval, X. Niu, S. J. May, R.W. Collins, and C. R. Wronski, 17th European PV Solar Energy Conf. Proc., 3, 2842 (2002).

[18] J. Pearce, X. Niu, R. Koval, G. Ganguly, D. Carlson, R.W. Collins, C.R. Wronski, Mat. Res. Soc. Proc., 664, A12.3 (2001).